

Case Studies of Exocomets in the System of HD 10180

Birgit Loibnegger¹, Rudolf Dvorak¹, Manfred Cuntz²

¹Institute of Astronomy, University of Vienna, Türkenschanzstr. 17
A-1180 Vienna, Austria

`birgit.loibnegger@univie.ac.at; rudolf.dvorak@univie.ac.at`

²Department of Physics, University of Texas at Arlington,
Arlington, TX 76019, USA

`cuntz@uta.edu`

Received _____; accepted _____

ABSTRACT

The aim of our study is to investigate the dynamics of possible comets in the HD 10180 system. This investigation is motivated by the discovery of exocomets in various systems, especially β Pictoris, as well as in at least ten other systems. Detailed theoretical studies about the formation and evolution of star–planet systems indicate that exocomets should be quite common. Further observational results are expected in the foreseeable future, in part due to the availability of the Large Synoptic Survey Telescope. Nonetheless, the Solar System represents the best studied example for comets, thus serving as a prime motivation for investigating comets in HD 10180 as well. HD 10180 is strikingly similar to the Sun. This system contains six confirmed planets and (at least) two additional planets subject to final verification. In our studies, we consider comets of different inclinations and eccentricities and find an array of different outcomes such as encounters with planets, captures, and escapes. Comets with relatively large eccentricities are able to enter the inner region of the system facing early planetary encounters. Stable comets experience long-term evolution of orbital elements, as expected. We also tried to distinguish cometary families akin to our Solar System but no clear distinction between possible families was found. Generally, theoretical and observational studies of exoplanets have a large range of ramifications, involving the origin, structure and evolution of systems as well as the proliferation of water and prebiotic compounds to terrestrial planets, which will increase their chances of being habitable.

Subject headings: astrobiology — circumstellar matter — comets: general — methods: numerical — protoplanetary disks — stars: individual (HD 10180)

1. Introduction

Comets appear to constitute a crucial component of many (or most) star–planet systems as informed by the structure of the Solar System as well as observations of the environments of stars other than the Sun. There are also theoretical studies, which tend to indicate that comets might be a quasi-universal phenomenon, especially regarding the environments of solar-type main-sequence stars (see below). As identified in the Solar System, comets are relatively small icy objects, often only a few kilometers in extent (i.e., ~ 0.1 to ~ 100 km in diameter) that formed in the outer Solar System where temperatures have been (and still are) sufficiently low to allow for frozen water. Comets thus represent leftovers from the early Solar System, closely associated with its formation process (Brasser 2008; Cook et al. 2016).

This picture has detailed implications for Earth (and possibly Mars, if considered in an exobiological context). Based on detailed studies on the early history of the Solar System, the inner part of the protostellar disk, due to its proximity to the Sun and hence shaped by both high temperatures and high solar wind pressure, contained a relatively high concentration of silicates and heavy elements. On the other hand, icy particles and water in notable quantities could only have existed relatively far away from the Sun (e.g., Martin & Livio 2014). Considering that the Earth is assumed to have formed in the inner, dry part of the disk (e.g., Martin & Livio 2014; Rubie et al. 2015), most of its water had to be delivered to it (and to Mars) from beyond the snowline, i.e., ~ 3.1 au (Martin & Livio 2012).

Nonetheless, underlying scenarios, including those considering the efficiency of water transport by planetesimals, asteroids and comets, are still subjects of ongoing research (see Genda & Ikoma 2008). Recent observations of comets (e.g., Hartogh et al. 2011; Altwegg et al. 2015) reinforce that the D/H ratio of the Solar System comets agrees

with or exceeds the D/H ratio found in Earth’s oceans. Bockelée-Morvan et al. (2012) measured, by using the *Herschel Space Observatory*, the $^{16}\text{O}/^{18}\text{O}$ and D/H ratios for the Oort Cloud comet C/2009 P1 (Garradd), whereas Altwegg et al. (2015) focused on 67P/Churyumov-Gerasimenko, a Jupiter family comet. Another pivotal aspect of that latter comet is its organic-rich surface as seen by *VIRTIS/Rosetta* (Capaccioni et al. 2015; Rickman et al. 2015). Note that some of these concepts, including those based on results from spectroscopy, are also relevant for studies beyond the Solar System.

There are also significant findings based on theoretical work. Stern (1990), for instance, assumes that comets are a natural product of planetary system formation as is the Oort Cloud. Simulations of planet formation for our own Solar System show that during the formation process of the gas giants frequent ejection of icy planetesimals from the planetary region took place. Some of those led to the formation of the Oort Cloud while most of them escaped to the interstellar space. Based on the Nice model of planet migration, Brasser (2008) investigated the possible two-stage formation of the Oort Cloud in the Solar System. Their model showed a possible mass for the outer Oort Cloud in the range of 0.5 to to 1 M_{\oplus} with a most likely value close to 0.9 M_{\oplus} , in agreement with observational estimates. This finding is also relevant for the possibility of comets in exosolar systems.

In fact, it is noteworthy that pivotal evidence has been obtained that comets exist around stars other than the Sun as well; they are also referred to as exocomets or Falling Evaporating Bodies (a somewhat more generic term). The first system named to harbor exocomets is β Pictoris, an A6 main-sequence star. Beust et al. (1990) were first to analyze the metallic absorption lines found in the stellar spectrum and to create a model of evaporation, which fitted the behavior of the Ca II. They argued that frequent infalls could be the result of a perturbing action of an (at that time) protoplanetary body embedded in the disk. Furthermore, they related the dynamics of the exocomets-as-indicated to a major

planet in the β Pictoris system, which was not known at the time, but has been found later (β Pictoris b).

A larger array of observational results regarding comets in the β Pictoris system has recently been given by Kiefer et al. (2014). This work made use of more than 1,100 spectra (Ca II H, K) obtained between 2003 and 2011 by the HARPS (*High Accuracy Radial velocity Planet Searcher*) instrument. In fact, as described by the authors, the β Pictoris system appears to contain two families of exocomets, i.e., one consisting of exocomets producing shallow absorption lines, attributable to old exhausted comets trapped in a mean motion resonance with a massive planet (as previously indicated by Beust et al. (1990)), and one family of relatively recent comets associated with the fragmentation of one or a few parent bodies. Based on results by, e.g., Zuckerman & Song (2012) and Welsh & Montgomery (2013), comets have also been found in other exoplanetary systems as well. One example is 49 Ceti, a relatively young (40 Myr) A-type main-sequence star. Additional examples are HD 21620, HD 42111, HD 110411, HD 145964, and HD 183324 (among others), which increases the total number of stars with indications of exocomets to (at least) 10. Several of these cases have been identified by Welsh & Montgomery (2013) who studied Ca II K absorption profiles from 21 nearby A stars with circumstellar gas debris disks. They found weak absorption features, which appear only sporadically and show radial velocities in the range of $\pm 100 \text{ km s}^{-1}$, which the authors interpret as firm indications of exocomets. The indicated exocomets are around mainly young stars ($\sim 5 \text{ Myr}$); these stars are supposedly in the phase of planet formation.

There are also significant astrobiological implications to the study of exocomets, which are closely related to the possible habitability of terrestrial planets in exosolar systems. A highly significant aspect is that exocomets are able to deliver both liquid water and basic organic substances from regions beyond the snowline to the inner domains of star-planet

systems where terrestrial planets with features in supportive to habitability reside; see, e.g., observational results and analyses for 67P/Churyumov-Gerasimenko by Capaccioni et al. (2015) and Rickman et al. (2015) based on *Rosetta*. Recently, Bosiek et al. (2016) argued that the ability of comets and comet-like asteroids to foster prebiotic chemistry as well as their available energy may be relevant for facilitating habitability in various exosolar systems.

A more stringent perspective has previously been conveyed by Wickramasinghe et al. (2009) and Wickramasinghe (2010). They discussed the possible existence of liquid water in comets, including the general potential for panspermia (e.g., Hoyle & Wickramasinghe 1986; von Bloh et al. 2003). Based on the temperature and radiative environments, transient melting in comets in inner stellar systems might be able to occur. Supposed that comets were seeded with microbes at the time of their formation from prebiotic material, Wickramasinghe et al. (2009) conjectured that there would be sufficient time available for exponential amplification and evolution within the liquid interiors. From a terrestrial point of view, certain kinds of extremophiles have been identified (e.g., Rothschild & Mancinelli 2001), which could potentially exist and flourish in such extreme environments.

The general aspect of our work is to explore based on theoretical orbital simulations whether in exosolar systems as, e.g., HD 10180 (where the center star has properties akin to the Sun) comets happen to exist in different families similar to the ones observed in the Solar System, namely, the Halley comets (HC) and the Jupiter family comets (JFC). However, it turned out that for HD 10180 no clear separation of cometary families could be identified. In Section 2, we discuss our theoretical approach, including comments about the HD 10180 system itself with focus on the Neptune-type planets considered for our time-dependent simulation. We also describe the methods as used and the numerical set-up. Our results and discussion are given in Section 3. Finally, in Section 4, we present the

summary and conclusions of our work.

2. Theoretical Approach

2.1. The HD 10180 System

HD 10180 is located in the southern-sky constellation of Hydrus at a distance of 39.0 ± 0.6 pc from the Sun (van Leeuwen 2007). Based on the *Hipparcos* catalog (ESA 1997), the stellar spectral type is given as G1 V (Nordström et al. 2004), which makes HD 10180 an almost-twin to our Sun (G2 V). The stellar effective temperature is given as 5911 ± 19 K, and its luminosity and mass are identified as $1.49 \pm 0.02 L_{\odot}$ and $1.06 \pm 0.05 M_{\odot}$, respectively; see Lovis et al. (2011) and references therein. Based on the star’s level of chromospheric activity, the age of HD 10180 was determined as 4.3 ± 0.5 Gyr (Lovis et al. 2011), which is (within its error bar) in agreement with the age of the Sun.

Lovis et al. (2011) conducted a high-precision radial velocity survey with the HARPS spectrograph, which led to the discovery of a planetary system consisting of at least five Neptune-mass planets with minimum masses ranging from 12 to $25 m_{\oplus}$ (i.e., planet c, d, e, f, and g). They also found tentative evidence for an inner Earth-mass planet (HD 10180 b) with a minimum mass of $1.35 \pm 0.23 M_{\oplus}$ as well as more substantial evidence for an outer, more massive planet (HD 10180 h) with a minimum mass of $65 m_{\oplus}$ located at a distance of $3.42^{+0.12}_{-0.13}$ au, and with an approximate orbital period of 2248 days; see Table 1 for details. In a succeeding study, Tuomi (2012) found two statistically significant signals corresponding to two additional planets in close circular orbits (i.e., HD 10180 i and HD 10180 j) with $67.55^{+0.68}_{-0.88}$ and $9.655^{+0.022}_{-0.072}$ day periods and minimum masses of $5.1^{+3.1}_{-3.2} m_{\oplus}$ and $1.9^{+1.6}_{-1.8} m_{\oplus}$, respectively, indicatives of super-Earths.

Tuomi (2012) also confirmed the existence of the five Neptunian planets (with minor revisions concerning the previously reported parameters) as well as the existence of HD 10180 h and found evidence for two additional planets. Thus, based on the work by Lovis et al. (2011) and Tuomi (2012), it can be concluded that HD 10180 is a tightly packed system with six or possibly nine planets; eight of those are spaced between 0.02 and 1.42 au from the star and another planet is located at ~ 3.40 au. If all of these planets are verified, it would make HD 10180 the present-time record holder with more planets in orbit than there are in the Solar System! Note that the semi-major axes are fairly regularly spaced on a logarithmic scale, thus exhibiting an approximate Titius-Bode-type law. Other examples of planetary systems exhibiting quasi-logarithmic spacing have previously been explored by, e.g., Cuntz (2012) and Bovaird & Lineweaver (2013). Lovis et al. (2011) also commented on possible formation scenarios of the HD 10180 system in the view of the planetary spacing and mass distribution.

Reasons for us to choose HD 10180 as system of study include the striking similarity of the host star to the Sun and, even more importantly, the system’s general composition: The most massive planet HD 10180 h is located outside of all other planets at a distance of ~ 3.4 au from the central star with a mass of $\sim 64.4 m_{\oplus}$; all inner planets, including the five Neptunian planets have masses $m < 26 m_{\oplus}$ and four of them orbit inside of 1 au. Although there are notable differences to the Solar System, there are general properties where the system of HD 10180 and that of the Sun agree: in the Solar System, Jupiter, the most massive planet ($317.8 m_{\oplus}$), acts as the main perturber for asteroidal and cometary objects, thus deflecting them to reach the terrestrial planets located inside of its orbit. Therefore, in the HD 10180 system, we expect HD 10180 h to play a similar role resulting in deflecting and capturing comets.

In Table 2, further information is given about the four outer planets HD 10180 e to h

considered in our computations. The Hill radius of HD 10180 h extends to 20×10^6 km (i.e., 53 times the Earth–Moon distance). Jupiter in our Solar System, with a semi-major axis of 5.2 au and about 4 times the mass of HD 10180 h has a Hill radius $R_{\text{Hill}} \simeq 52 \times 10^6$ km. In the following, two different densities are assumed for the planets of HD 10180, which are: $\rho_1 = 1 \text{ g cm}^{-3}$ and $\rho_2 = 2 \text{ g cm}^{-3}$; the assumed density values are relevant for investigating close comet–planet encounters. Here ρ_1 is set to be very close to the numerical average between the densities¹ of Jupiter and Saturn, whereas ρ_2 is chosen as the approximate upper limit of medium-sized gas planets as, e.g., Neptune. The choices for ρ_1 and ρ_2 are also consistent with empirically deduced values for gaseous exoplanets obtained by Guillot (1999) and subsequent work.

2.2. Methods and Numerical Setup

Guided by the structure of the Solar System, we assume that the system of HD 10180 might also harbor an Oort-type cloud of comets far from the star, and perhaps other comets in closer stellar vicinity (i.e., comets up to 1000 au from the star and Kuiper belt comets). It is further assumed that every now and then the comets are gravitationally disturbed by, e.g., a passing star or a cloud of interstellar matter. The focus of our study is to investigate how those comets are disturbed or captured by one of the close-in planets, or even forced to escape from the system. When referring in our study to comets as captured, we address comets that are for a certain timespan in an orbit of small eccentricity and semi-major axis.

Our computations take into account a total of four planets (see Table 1), considering that the inner planets (with the closest planet having a semi-major axis of only $a \simeq 0.06$ au)

¹ For comparison: Jupiter: 1.326 g cm^{-3} , Saturn: 0.687 g cm^{-3} , and Neptune: 1.638 g cm^{-3}

are not expected to noticeably change our statistical results. A more comprehensive approach based on additional planets would be without an obvious impact on the outcome, as our test computations have shown. It is evident that the outermost planet (i.e., HD 10180 h), considered in our simulations, is expected to be the dominant planet affecting the exocomets’ orbital motions, a role played by Jupiter in the Solar System.

In our study, we used extensive numerical integrations for tens of thousands of fictitious comets (assumed as massless) for the HD 10180 system. The method of integration for the equations of motion is based on Lie-transformation, which is known to be a fast and efficient tool. This method has been successfully used since many years for different problems in astrodynamics (e.g., Dvorak 1986). Comparisons with other methods have shown that this method is especially adapted to model close encounters of celestial bodies as well as collisions. The reason is that this method utilizes an automatic step-size control connected to the chosen precision selected for solving the differential equations (e.g., Eggl & Dvorak 2010); it was also compared to other methods in numerous ways.

Our integration scheme encompasses the central star of the HD 10180 system, the four system’s outer planets (see Table 1) as well as 100 fictitious exocomets at an initial distance of $a = 89$ au, assumed as massless. The comets were assumed to originate from an Oort Cloud analogue and therefore have been placed in nearly hyperbolic orbits. The initial semi-major axis of 89 au was chosen to be close enough to allow interactions with the system’s inner planets, but, on the other hand, also set to be well beyond the outermost system planet, HD 10180 h. Different initial semi-major axes were used in test simulations for some of the initial conditions. However, no discernible differences in the final statistics for the comets were found.

The initial inclinations and eccentricities are chosen as follows: initial inclinations from the plane ($i = 1^\circ$) with $\Delta i = 10^\circ$ extending till retrograde orbits for 100 different perihelion

longitudes and initial eccentricities ranging from $e_0 = 0.905$ to 0.99. Furthermore, the longitude of the ascending node Ω was set to the same angle as the inclination and the mean anomaly M was always set to 1° . With these choices of initial conditions the number of integrated fictitious cometary orbits was more than 30,000, namely $19 (i) \times 100 (\omega) \times 16 (e)$ and we were able to cover all the possible directions of incoming comets (see Fig. 2). The integration time was set to 1 Myr; in a few cases of special interest, we continue to 5 Myr (see Fig. 3 and 4).

It could be argued that in our Solar System many of the comets have orbits of low inclination — so why consider an isotropic influx of comets in HD 10180? The reason is that without detailed information of possible exocomets in that system, an isotropic angular distribution for the initial conditions appears to be the most appropriate default assumption. Figure 1 shows the distribution of comets in the inner Solar System on hyperbolic or nearly parabolic orbits, which can then be readily observed. The results from the SOHO satellite are indicating that there are two cometary families: the Kreutz sungrazers as well as the Meyer group of comets. Other comets entering the Solar System seem to be randomly distributed over the sphere. As part of our study, we wish to identify the prevailing patterns of comets for HD 10180.

During orbital evolution, the orbits of the exocomets undergo close encounters with the planets. This behavior sometimes led to captures into low-eccentric orbits (see Fig. 3 and 4) or to ejections from the system; in a few cases, collisions with the host star occurred. Whenever a comet was ejected from the system, we inserted another one with the same ‘initial’ conditions as the escaper. Since at the time of insertion the configuration of the planets has changed, the newly inserted comet will exhibit a different dynamics. Based on this procedure, we will always keep the number of fictitious exocomets equal to 100.

As part of our numerical simulation, we counted the unstable comets for the various

eccentricities and inclinations; the respective values are shown in Fig. 5. If all comets stayed on stable orbits — they could still be captured as periodic comets (e.g., Fig. 7) or assume a chaotic but still stable orbit — the number of ejected comets in the respective table is zero. Figure 5 shows very well the regime of stable orbits for comets of initial inclinations $100^\circ < i < 160^\circ$ and eccentricities $e_0 < 0.99$ surrounded by areas of initial conditions where many orbitally unstable comets found.

3. Results and Discussion

3.1. General Case Studies

By making use of Lie-series (see, e.g., Gröbner 1960; Stumpff 1974; Dvorak et al. 1983; Delva 1984; Eggl & Dvorak 2010, for background information) close encounters of the incoming comets with the planets are calculated with a sufficiently high precision. Due to close planetary encounters, some of the comets are captured, whereas others are ejected from the system. In the Solar System, captured comets form families due to the gravitational influence of Jupiter. Our simulations show that the outermost planet (i.e., HD 10180 h) is able to change the orbits of incoming comets most profoundly when arriving with high speeds from the outskirts of the system. Moreover, close encounters also occur with respect to the inner planets as considered (see Table 1).

The number of ejected comets increases more significantly for comets of larger eccentricities and smaller inclinations, owing to the fact that (1) for smaller inclinations, the number of encounters and consequently escapers is larger and (2) with larger eccentricities, there is an increased likelihood that the comets enter the inner region of the system and undergo relatively early encounters resulting in escape.

The combined preliminary results for inclinations from $i_0 = 0^\circ$ to 90° are shown in

Tables 3 and 4 (prograde orbits), as well as in Table 5 from $i_0 = 100^\circ$ to 170° (retrograde orbits) and in Fig. 5. It is found that for large eccentricities many more escapes from the system occur. The border between completely stable and escaping orbits is not a sharp one; in fact, at the interface separating the two regions, there is a small band characterized by statistical number fluctuations. However, there are no escapers for retrograde orbits up to $e_0 = 0.94$; hence, we don't show this regime in a separate table. Also, this 'mixed' band is still under investigation, as well as the computations for $i_0 = 180^\circ$. But even when there is no immediate crossing of the cometary orbit with the planet, the impact of secular resonances can lead to changes in a comet's orbit that close encounters with the planets are possible. Figure 6 reveals that the orbit for $e_0 = 0.935$ (dark blue line) is in terms of its perihelion distance still far away from the orbit of HD 10180 h (> 2 au), but nevertheless at a later time, this orbit is changed so that close encounters with the planets lead to the comet's escape from the system. Table 3 shows that a total of 104 comets have been ejected from the system (first line for $i_0 = 0^\circ$ and $e_0 = 0.935$).

In Fig. 9 to 11 we show orbital properties of comets populating orbits of capture, depending on their initial conditions. Only for a few cases it is possible that comets of initially planar orbits are also spread to retrograde orbits as the simulations progress. The different values of the initial eccentricities depicted in the figures are $e_0 = 0.99, 0.98, 0.975$, and 0.965 . Together with the chosen semi-major axis of $a = 89$ au, these values make those comets immediately to possible planet HD 10180 h ($a = 3.4$ au) crossers. The encounters with the planets force the comets into either ejected orbits or captured ones.

The effect of the most massive planet, HD 10180 h (see Table 1), on comet scattering seems obvious. Nonetheless, the second massive planet, HD 10180 g, located at about half the distance from the star, could potentially also have a non-negligible influence on cometary orbits. This can be seen in the graphs of Fig. 8, which show the main outcome

of our simulations. In the *lower left panel* of Fig. 8 (integration done without planet HD 10180 h) and Fig. 8 *upper right panel* (integration done without planet HD 10180 g) the differences are well pronounced. When planet h is excluded, only the comets with initial eccentricity of $e > 0.98$ are able to reach the orbit of planet g and thus get scattered and ejected from the system. The influence of planet g, on the other hand, is not that big. Comparing the two *upper panels* of Fig. 8 shows that they look almost identical, which means that taking out planet g does not have a noticeable effect on the scattering process. Nevertheless, there is still a difference in the maximal number of ejected comets. Taking out planet g reduces the total number of ejected comets. Integrating the system for 5 Myr (shown in Fig. 8 in the *lower right panel*) demonstrates that only the total number of ejected comets increases. However, the overall picture of stability does not noticeably change from a statistical point of view. Comets with initially high eccentricity and low inclination $e_0 > 0.5$ and $0^\circ < i_0 < 40^\circ$ tend again to become unstable, whereas the main regime of initial conditions (e_0, i_0) leads to stable cometary orbits. These comets stay in the system for the entire integration time of 5 Myr.

Figures. 9 to 11 show the properties of captured comets based on 1 Myr computations by depicting various orbital elements, which are: eccentricity, semi-major axis, and inclination (see color code). While for Fig. 9 all 4 planets were included, planet g was excluded from the simulations depicted in Fig. 10 and planet h was excluded for the simulations of Fig. 11. It is found that the difference in the scattering outcome for Fig. 9 and Fig. 10 is relatively minor. Comets with eccentricities as shown are able to reach the inner parts of the planetary system and interact with the planets; in fact, they are scattered to orbits with eccentricities of $e < 0.6$ and semi-major axis as small as 5 au. Interestingly, the inclinations of the final orbits of comets can remain high, especially for comets with initially high eccentricities. This behavior is revealed by the orange color of the dots in the *lower right panel* of Figs. 9 and 10.

Fig. 11, however, indicates a completely different outcome. For the integrations as depicted, planet h has been excluded from the computations. It can be seen that comets of relatively low initial eccentricity ($e_0 = 0.965$) are unable to reach the orbit of planet g, which is now the outermost planet able to influence the orbits of incoming comets. Thus, the comets stay on their highly eccentric orbits far away from the planetary system. Increasing the initial eccentricity shows that comets can now approach planet g and can be scattered to orbits farther inward, i.e., $a < 60$ au. Note that only comets with an eccentricity as high as 0.99 can be scattered to orbits with $e < 0.6$ and $a < 5$ au. Nevertheless, the number of comets ending up in such orbits is small compared to the number of comets based on the integration for the whole system versus the system with planet g excluded. This leads again to the conclusion that the influence of the most massive planet h on comet scattering is clearly dominant.

Furthermore, when considering the interval of $0.1 < e < 0.7$ in Figs. 9 and 11, one can see that with planet h included, more comets are scattered into orbits with an eccentricity of that range. However, with planet h excluded, the comets are not able to reach a planetary orbit, which would influence them gravitationally and scatter them to orbits of smaller eccentricity (see Fig. 11). The significant influence of planet HD 10180 h on the scattering of the comets, especially on comets of higher initial inclination, can be explained by the size of its Hill sphere. Due to its bigger mass and its orbit, the Hill sphere of planet HD 10180 h has a radius of 0.1379 au, which is more than three times larger than that of planet g, given as 0.04 au (see Table 2).

Moreover, comets interacting gravitationally with planet h have a lower velocity, which results in a longer period during which planet h is able to affect the comet's orbit. Comets encountering planet g are closer to their perihelion and thus have a higher velocity, which further reduces the duration of stay in the sphere of influence of planet g. Thus, taking out

planet HD 10180 h has a profound influence on the scattering process. Additionally, it is found that the influence of planet g on the comets is relatively weak because of its position compared to planet h.

We also explored the probability of comets to be captured into orbits with moderate values for the semi-major axis and eccentricity, i.e., $e < 0.7$ and $a < 10$ au. This was done for two cases: first, with all four planets included in the calculations (see Fig. 12) and second, for a system with planet HD 10180 h excluded (see Fig. 13). It was found that the highest probability of capture occurs for comets with an initial eccentricity between $e_0 = 0.985$ and 0.97 combined with an initial inclination close to 0° . The next highest peak, albeit significantly lower, was found for comets with an initial inclination of 30° . Furthermore, for comets with initial eccentricities below 0.97 , no significant captures occurred. Additionally, it was found that the overall picture did not change much when excluding planet h, except that for comets with an initial eccentricity of 0.985 the small peaks showing a capture probability of $\sim 5\%$ for comets with an initial inclination of 30° , 90° , and 120° disappeared. Hence, we conclude that planet g is responsible for the capture of comets with this particular initial condition.

3.2. A Very Special Capture

Next we discuss an example of a captured exocomet in more detail (see Fig. 3 and 4). Although the ordinary integration time has been set to 1 Myr, we have chosen an extended time of up to 5 Myr for orbits exhibiting features of particular interest. This example has also been chosen because of a secular resonance, which is still under further investigation; see Lhotka et al. (2016).

It is found that the comet’s semi-major axis decreases drastically within several 10^5 yrs

from $a = 45$ au to $a = 5$ au (see *blue* line in Fig. 4). Additionally, within the same time interval ($\tau < 1$ Myr) the comet’s eccentricity drops from almost parabolic ($e \simeq 1.0$) to close to circular ($e \simeq 0.0$) (*green* in Fig. 3). Thereafter, the comet’s semi-major axis increases within a relatively short time frame to up to about $a = 15$ au, followed by some fluctuations between 9 and 15 au (*blue* in Fig. 4). The decrease of the comet’s semi-major axis (shown in *blue* in Fig. 4) can be explained by jumping from one resonance to another. Note that the same behavior was previously observed for the Solar System comet Halley (Dvorak & Kribbel 1990).

Subsequently, the semi-major axis settles at $a = 13$ au due to a close encounter with planet HD 10180 b at 1.3 Myr. In the next 1 Myr, no significant changes occur in the comet’s orbital elements. During this quiet time (i.e., $1.3 \text{ Myr} < \tau < 2.3 \text{ Myr}$) the eccentricity undergoes only small variations (*green* in Fig. 3). In the same figure we depict the perihelion distance (*blue* line) for this time interval showing smooth changes from $q = 3.4$ to 5.5 au; this is a safe zone void from any encounters. At the end of this stage (i.e., $\tau = 2.3 \text{ Myr}$), the comet approaches the planet HD 10180 h again ($q = 3.4$), which transforms the comet’s orbit into a chaotic one.

During the time interval ahead (i.e., $3.1 \text{ Myr} < \tau < 3.8 \text{ Myr}$), the comet experiences only small changes regarding three dynamic properties, i.e., the semi-major axis a (*blue* line in Fig. 4), the eccentricity e (*green* in Fig. 3), and the inclination i (*green* line in Fig. 4). After several close encounters with HD 10180 g (not shown here) visible through large variations in all orbital parameters at approximately 3.9 Myr the comet enters into a more quiet regime. Another feature resulting in a relatively stable orbit occurs between 4.1 Myr and 4.8 Myr. In this case, its semi-major axis is relatively small ($a \simeq 3.0$) with increasing values towards the end of that period.

Finally, we stop the integration after 5 Myr, a time when the inclination undergoes big

fluctuations between 25° and 55° for this comet. Detailed results are given in Fig. 3 and 4, with *red* marking the encounters with planet HD 10180 h in Fig. 3. Although sometimes the comet approaches the planet as close as ten planetary radii, no collisions are found to occur.

4. Summary and Conclusions

The purpose of this work is to explore the orbital dynamics of possible exocomets in the HD 10180 star–planet system. Exocomets appear to constitute a significant component of stellar systems as informed by previous theoretical and observational studies. Besides the Solar System, the best studied case so far is β Pictoris (Kiefer et al. 2014), which appears to host two families of comets of different histories and degrees of fragmentation. Additional findings have been reported for at least 10 other stars (e.g., Zuckerman & Song 2012; Welsh & Montgomery 2013), with most of them being relatively young and possibly in the stage of planet formation. Continuing observational results are expected from the forthcoming *Large Synoptic Survey Telescope*².

Previous theoretical work about the detectability of exocomets include estimates by Hainaut (2011), who scaled realistic and extreme cases of the Solar System to the distance of neighboring stars. Cook et al. (2016) discussed the detectability of close interstellar comets in consideration of previous estimates by Moro-Martín et al. (2009); this study is expected to be helpful for future searches. Generally speaking, the study of exocomets, either belonging to the environments of stars or being interstellar in nature, carries significant information about planet formation and the prospects of habitable domains. Current work mostly focuses on young A-type stars (e.g., Zuckerman & Song 2012; Welsh & Montgomery

²See <https://www.lsst.org/>.

2013), but more comprehensive search missions are anticipated in the foreseeable future.

In the present work, we consider the system of HD 10180. The center star is of spectral type G1 V, and is strikingly similar to the Sun regarding mass, surface temperature, metallicity and age (Lovis et al. 2011, and references therein), with some of the data even agreeing with solar values within their error bars. Based on the work by Lovis et al. (2011) and Tuomi (2012) we know that the HD 10180 system is rich in planets as it may host up to nine planets (or even more, notwithstanding future detections), which makes it the present-time record holder, thus surpassing the Solar System. However, the planetary system of HD 10180 is much more compact than the Solar System. The outermost planet HD 10180 h has a distance from its star comparable to the big gap for Solar System asteroids between the 2:1 and 3:2 mean motion resonance with Jupiter.

Stern (1990) proposed that based on the detection rate of interstellar comets one could draw conclusions about the rate of planetary formation in the galaxy. In our study, we did not investigate the influence of planet formation or, e.g., the impact of giant planet migration on the comet ejection rates. Nevertheless, we found that due to gravitational interaction with the planets a substantial number of comets were ejected from the system, which allows us to conclude that not only planet formation mechanisms, but also the influence of passing stars with ensuing interactions of the comets with the planets and subsequent ejection from the system can account for a large number of interstellar comets (e.g., see Fig. 8 *lower right panel*).

Our simulations also showed that planet HD 10180 h dominates the cometary scattering process depending on the comets’ initial conditions. It is also governing the orbital dynamics of exocomets considered in our study; a feature also shared by Jupiter in the Solar System. Our simulations took into account more than 30,000 comets as part of the initial orbital integration scheme, which included comets of different initial eccentricity

and inclination (also encompassing comets in retrograde orbits). Our study shows different kinds of outcomes such as encounters with the planets, captures, escapes, and secular comet–planet resonances. The integration process itself included the four outer planets of the system, i.e., planet e, f, g, and h (see Table 1). Generally, comets with relatively large eccentricities were able to enter the inner region of the system, thus facing early close planetary encounters. Owing to our theoretical approach, the number of ejected comets considered in our simulation readily increased over time.

It was also found that for comets with large eccentricities many more escapes from the system occurred. However, the border between completely stable and escaping cometary orbits is not a sharp one; in fact, at the interface separating the two regions, there is a small band characterized by statistic fluctuations. Moreover, there are no ejections for retrograde orbits up to eccentricities of $e_0 = 0.94$. Nonetheless, even without crossings of cometary orbits with any of the planets, the impact of secular resonances can lead to changes in cometary orbits so that close planetary encounters are possible. We also showed how comets of initially planar orbits, in the context of our simulations, are spread evenly to also include retrograde orbits and could also be in long-term stable orbits around the host star (see Fig. 9).

Even though the idea of finding families of comets in the HD 10180 system was a key motivation for this work, we were unable to determine any dynamical families, although a very large number of captured comets has been identified through our numerical integrations. We think that the reason why no families of comets in the HD 10180 system were found is because of the system’s architecture, which aside from the many affinities to the Solar System still exhibits decisive differences. For example, in our system beyond the most massive planet Jupiter other massive planets exist able to influence the orbits of incoming objects, whereas in the HD 10180 system, the most massive planet h constitutes

the system’s outermost planet.

A particular focus of our work concerned the role of the comet’s initial eccentricity and inclination regarding capture, evolution of orbital elements, or the comet’s escape. In the future, we plan to extend our studies of comets to other exoplanetary systems including systems with compositions akin to the Solar System as well as systems with notably different structures. Moreover, we consider our work as part of the bigger picture associated with the study of comets, pertaining to the Solar System as well as to exosolar systems. Studies about exocomets yield a large range of implications, involving the origin, structure and evolution of systems as well as the proliferation of water and prebiotic compounds to terrestrial planets, which will increase their chances of being habitable. This latter aspect has been showcased by results from *Rosetta* (e.g., Capaccioni et al. 2015; Rickman et al. 2015; Bosiek et al. 2016), which indicate the pivotal role of comets regarding prebiotic chemistry and potential exobiology.

To consider the importance of exocomets for possible life in exosolar systems another possible extension of our future work will include the detailed study of encounters and collisions with planet HD 10180 g located at the outer edge of the system’s habitable zone, comparable to the position of Mars in the Solar System. This exosolar planet is Neptune-like; therefore, not being able to host life. However, an exomoon or a Trojan-type object associated with HD 10180 g could still be habitable.

This research is supported by the Austrian Science Fund (FWF) through grant S11603-N16 (B. L. and R. D.). Moreover, M. C. acknowledges support by the University of Texas at Arlington. We also thank an unknown referee for valuable advice allowing us to improve this paper.

REFERENCES

- Altwegg, K., Balsiger, H., Bar-Nun, A., et al. 2015, *Science*, 347, 387
- Beust, H., Vidal-Madjar, A., Ferlet, R., & Lagrange-Henri, A. M. 1990, *A&A*, 236, 202
- Bockelée-Morvan, D., Biver, N., Swinyard, B., et al. 2012, *A&A*, 544, L15
- Bosiek, K., Hausmann, M., & Hildenbrand, G. 2016, *Astrobiol.*, 16, 311
- Bovaird, T., & Lineweaver, C. H. 2013, *MNRAS*, 435, 1126
- Brasser, R. 2008, *A&A*, 492, 251
- Capaccioni, F., Coradini, A., Filacchione, G., et al. 2015, *Science*, 347, 628
- Cook, N. V., Ragozzine, D., Granvik, M., & Stephens, D. C. 2016, *ApJ*, 825, 51
- Cuntz, M. 2012, *PASJ*, 64, 73
- Delva, M. 1984, *Celestial Mechanics*, 34, 145
- Dvorak, R., Hanslmeier, A., & Lichtenegger, H. 1983, *BAAS*, 15 (3), 869
- Dvorak, R. 1986, *A&A*, 167, 379
- Dvorak, R., & Kribbel, J. 1990, *A&A*, 227, 264
- Eggl, S., & Dvorak, R. 2010, in *Dynamics of Small Solar System Bodies and Exoplanets*, eds. J. Souchay & R. Dvorak, *Lecture Notes in Physics*, Vol. 790 (Berlin: Springer), p. 431
- ESA 1997, *VizieR Online Data Catalog*, 1239, 0
- Genda, H., & Ikoma, M. 2008, *Icarus*, 194, 42

- Gröbner, W. 1960, *Die Lie-Reihen und ihre Anwendungen* (Berlin: Deutscher Verlag der Wissenschaften)
- Guillot, T. 1999, *Science*, 286, 72
- Hainaut, O. R. 2011, in *Molecules in the Atmospheres of Extrasolar Planets*, ed. J.-P. Beaulieu, S. Dieters, & G. Tinetti (San Francisco, CA: ASP), 450, 233
- Hanslmeier, A., & Dvorak, R. 1984, *A&A*, 132, 203
- Hartogh, P., Lis, D. C., Bockelée-Morvan, D., et al. 2011, *Nature*, 478, 218
- Hoyle, F., & Wickramasinghe, N. C. 1986, *Nature*, 322, 509
- Kiefer, F., Lecavelier des Etangs, A., Boissier, J., et al. 2014, *Nature*, 514, 462
- Lhotka, C., Dvorak, R., & Loibnegger, B. 2016, in preparation
- Lovis, C., Ségransan, D., Mayor, M., et al. 2011, *A&A*, 528, L112
- Martin, R. G., & Livio, M. 2012, *MNRAS*, 425, 6
- Martin, R. G., & Livio, M. 2014, *ApJ*, 783, 28
- Moro-Martín, A., Turner, E. L., & Loeb, A. 2009, *ApJ*, 704, 733
- Nordström, B., Mayor, M., Andersen, J., et al. 2004, *A&A*, 418, 989
- Nurmi, P., Valtonen, M. J., Zheng, J. Q., & Rickman, H. 2002, *MNRAS*, 333, 835
- Rickman, H., Marchi, S., A’Hearn, M. F., et al. 2015, *A&A*, 583, 44
- Rothschild, L. J., & Mancinelli, R. L. 2001, *Nature*, 409, 1092
- Rubie, D. C., Jacobson, S. A., Morbidelli, A., et al. 2015, *Icarus*, 248, 89

Stern, S. A. 1990, *PASP*, 102, 793

Stumpff, K. 1974, *Himmelsmechanik. Band 3: Allgemeine Störungen* (Berlin: Deutscher Verlag der Wissenschaften), p. 58

Tuomi, M. 2012, *A&A*, 543, A52

van Leeuwen, F. 2007, *A&A*, 474, 653

von Bloh, W., Franck, S., Bounama, C., & Schellnhuber, H. J. 2003, *Orig. Life Evol. Biosph.*, 33, 219

Welsh, B. Y., & Montgomery, S. 2013, *PASP*, 125, 759

Wickramasinghe, C. 2010, *IJAsB*, 9, 2

Wickramasinghe, J. T., Wickramasinghe, N. C., & Wallis, M. K. 2009, *IJAsB*, 8, 281

Zuckerman, B., & Song, I. 2012, *ApJ*, 758, 77

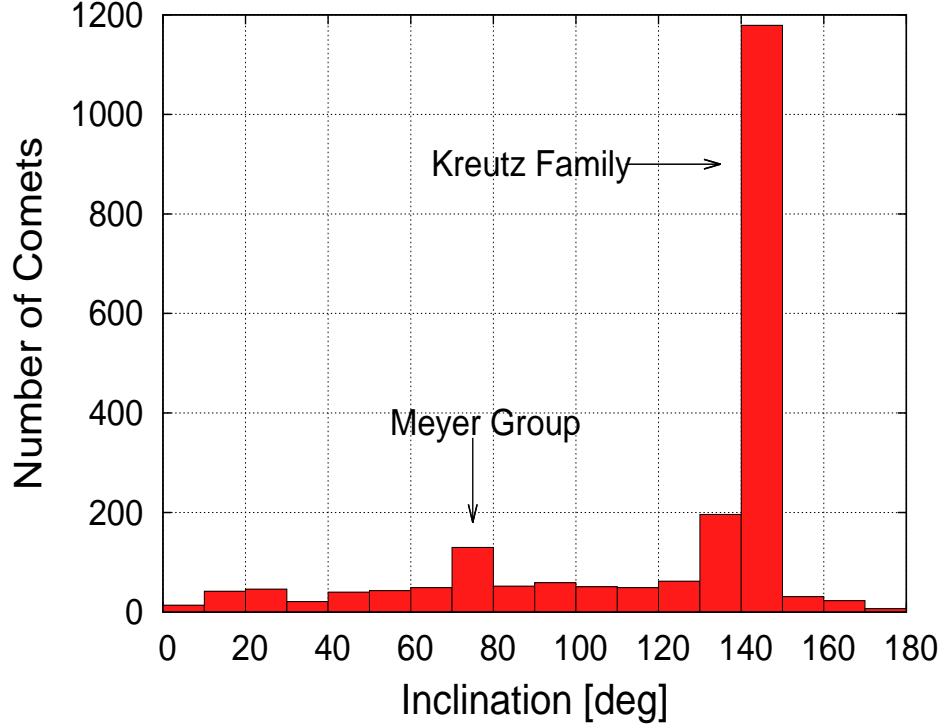


Fig. 1.— Distribution of comets in the Solar System with respect to their inclination on their hyperbolic or nearly parabolic orbits. The Kreutz family of comets is clearly visible as they all show an inclination around 145° . Except for this peak, all other inclinations show roughly the same numbers. Motivated by this result, our initial conditions for HD 10180 are also based on a spherical distribution of comets. See also Jssd.jpl.nasa.gov/sbdb-query.cgi for more information.

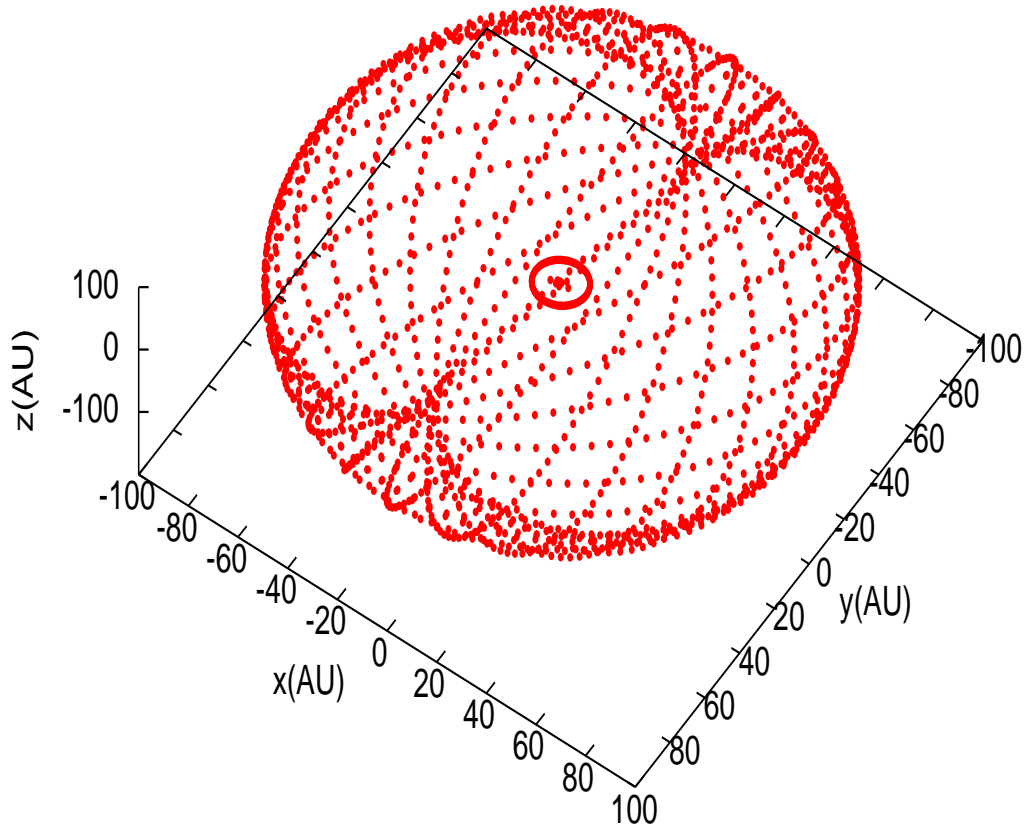


Fig. 2.— Initial distribution of comets from $i_0 = 0^\circ$ to 180° and $a = 89$ au in our integrations; the narrow ring close to the central star indicates the orbit of planet HD 10180 h.

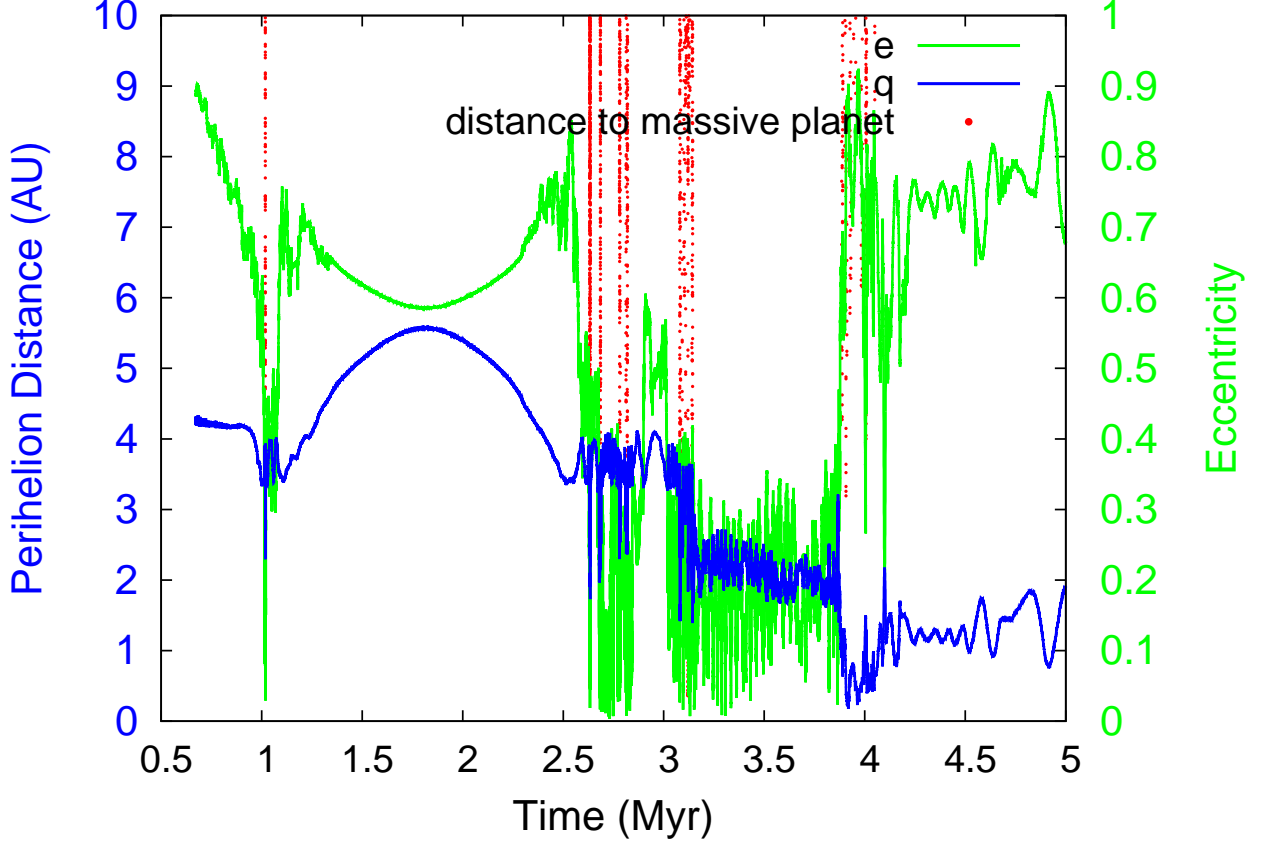


Fig. 3.— Time evolution for a particular example of a captured comet in the HD 10180 system. The y -axis shows the perihelion distance (blue), the eccentricity (green), and the close encounters with planet h (red) in units of its Hill radius (see Table 2). The stable period between 1 and 2.5 Myr is well pronounced. After this period, another time interval exhibiting low eccentricities follows. These periods are bounded by close encounters with the most massive planet in the system, planet h. Gravitational interactions during these encounters lead to visible changes in the cometary orbit.

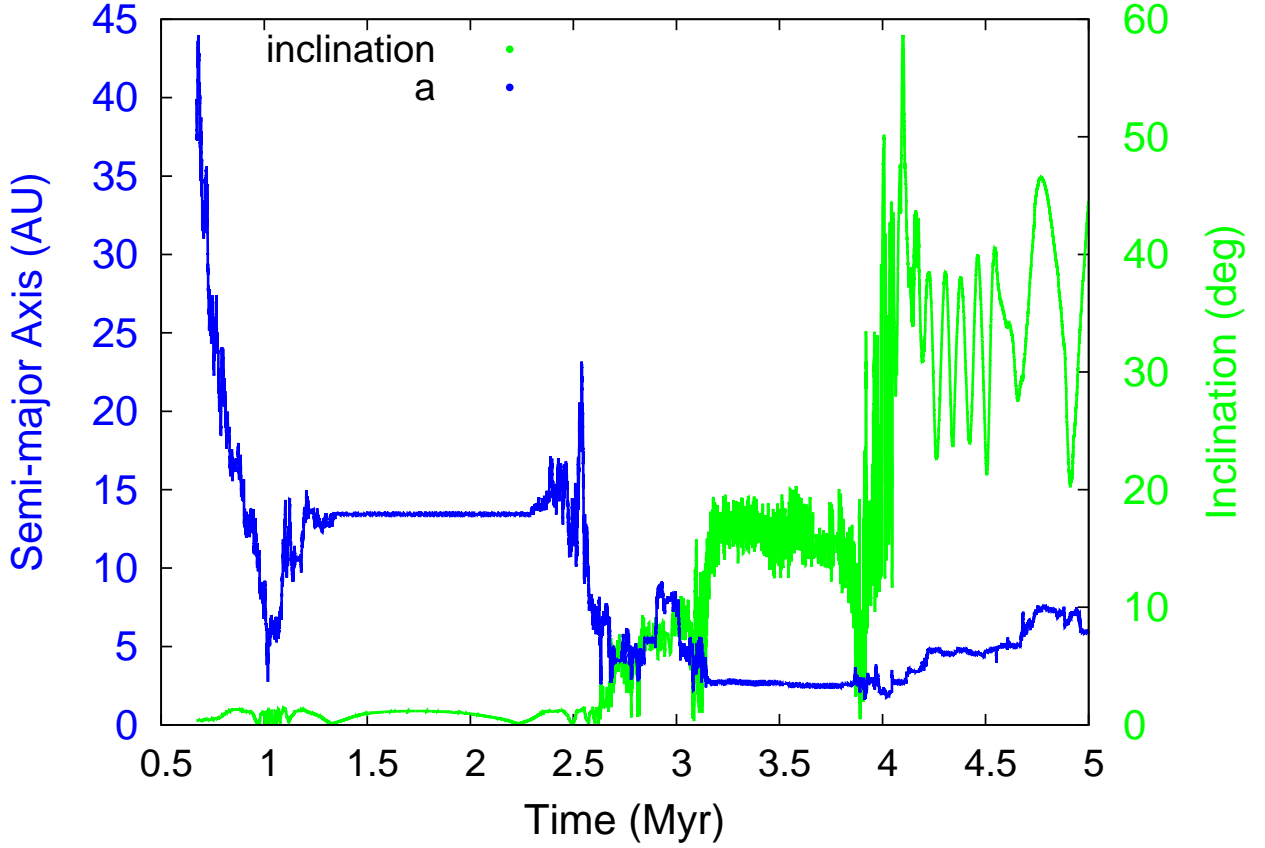


Fig. 4.— Time evolution for a particular example of a captured comet in the HD 10180 system. The y -axis shows the semi-major axis (blue) and the inclination (green). The comet enters the inner region and is captured in a stable orbit with $a \sim 14$ au for approximately 1.5 Myr (see also Fig. 3). Another stable period, even closer to the star (~ 4 au) follows. After a close encounter (see Fig. 3), the orbit becomes chaotic again and the comet may leave the inner planetary system once more.

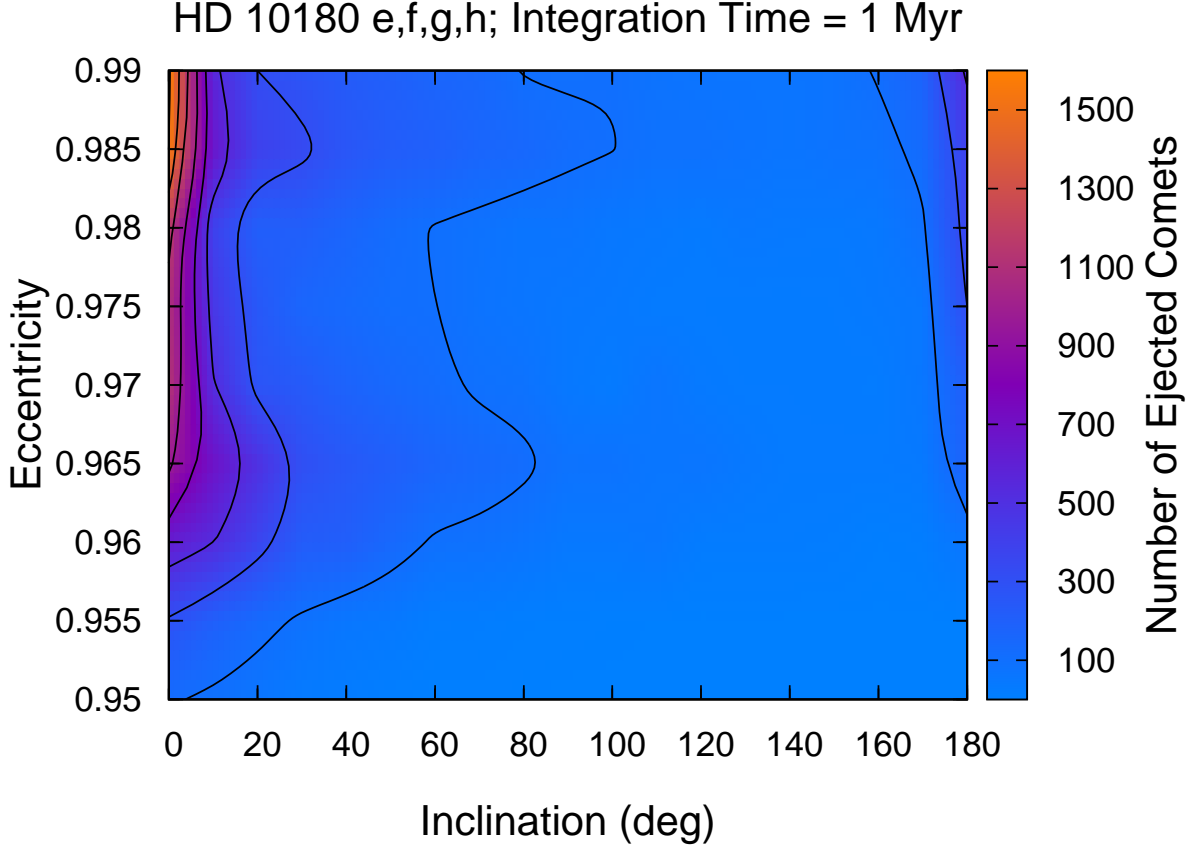


Fig. 5.— The color scheme indicates the number of ejected comets from the system for different initial conditions (e_0, i_0) and an integration time of 1 Myr. It is evident that for high initial eccentricities e_0 and low initial inclinations i_0 the number of ejected comets is highest. Furthermore, for higher inclinations the number of ejected comets — even those with high eccentricities — decreases. This means that comets starting with initial conditions in this regime tend to be stable for the entire integration time of 1 Myr.

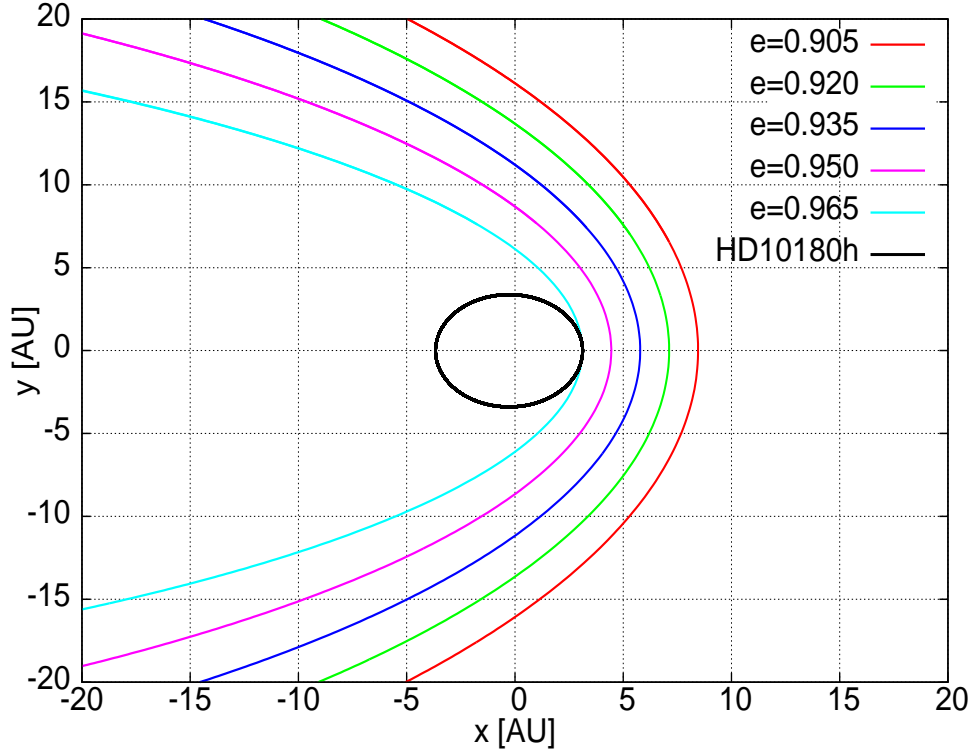


Fig. 6.— Depiction of five “safe” orbits for comets due to their initial conditions; the orbit of HD 10180 h is shown in black. Even with a high eccentricity of 0.965 (where the comet comes as close to the star as HD 10180 h), stable orbits are possible. However, as depicted in Fig. 5 — even with $e_0 > 0.95$, indicating that the perihelion distance of such a comet is still far away from the orbit of planet h — these comets are ejected.

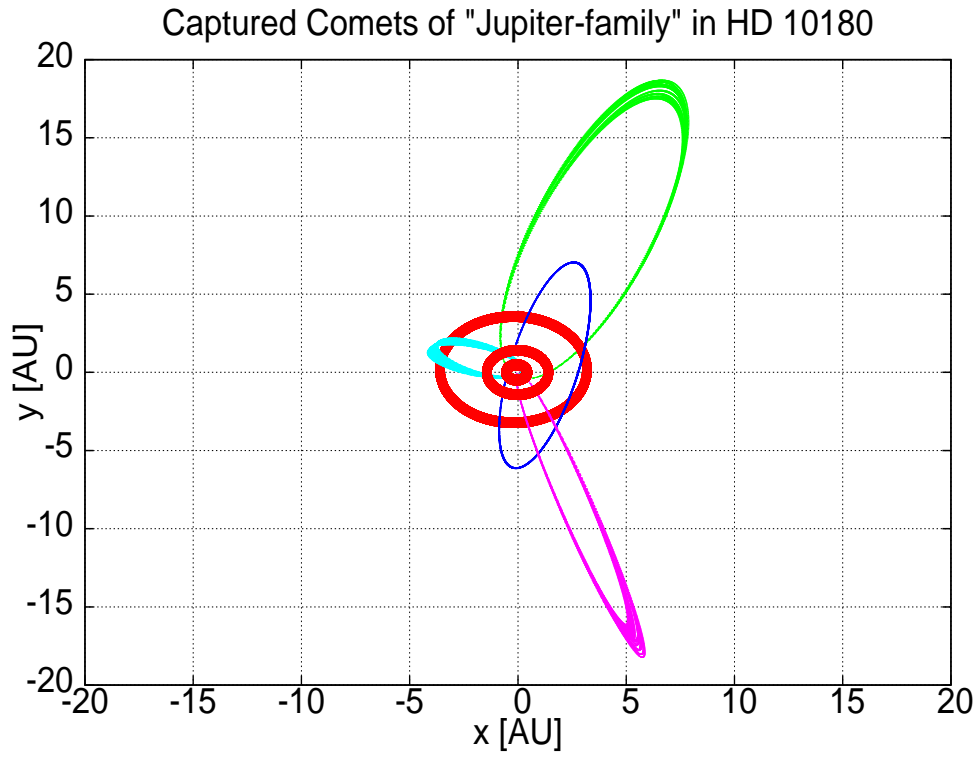


Fig. 7.— Orbits of four captured comets (in green, dark blue, light blue, and purple) together with the three outer planets HD 10180 f, g, and h (in red).

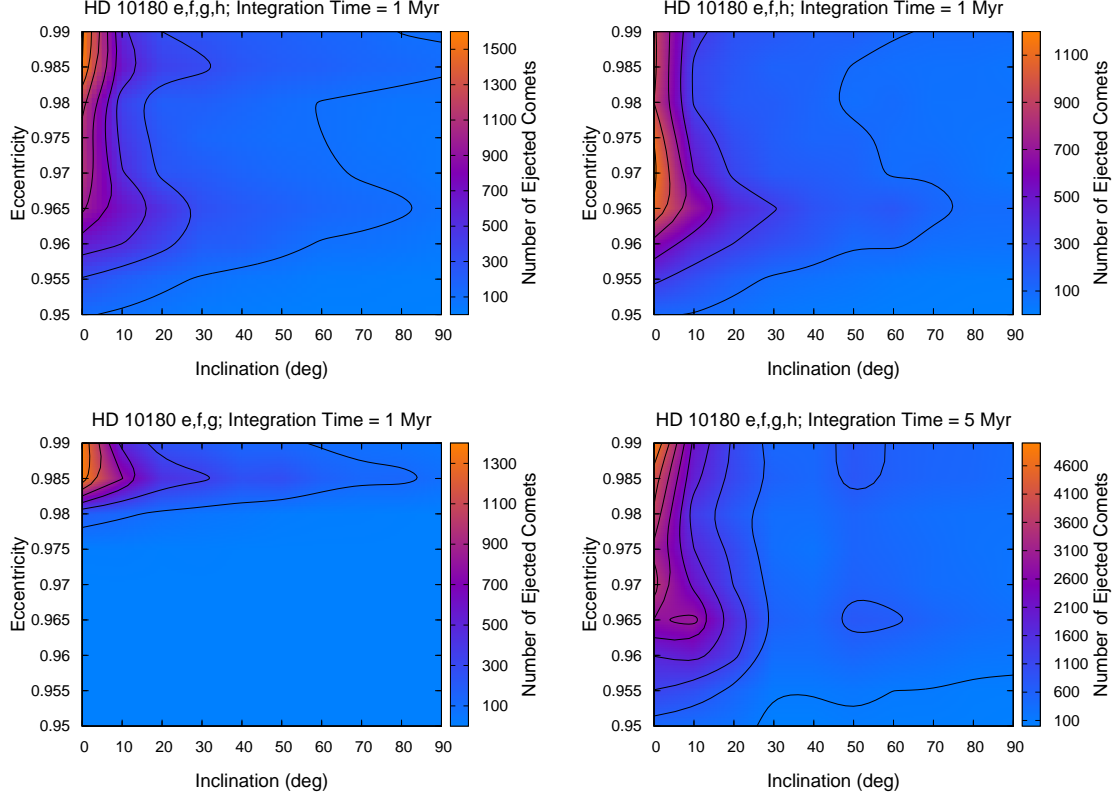


Fig. 8.— The color scheme indicates the number of escaped comets from the system for different initial conditions (e_0, i_0) and an integration time of 1 Myr for the different setups used: *Upper left*: Same as if Fig. 5, but here only shown for comets with initial inclination of up to 90° . The orange color in the left upper corner indicates that most of the comets with high eccentricity and low initial inclination are ejected from the system. *Upper right*: The exclusion of the second massive planet HD 10180 g does not really change the picture; see comparison to the *upper left* panel. The total number of comets ejected from the system is slightly smaller. Furthermore, the orange regime is shifted to comets with lower initial eccentricity. *Lower left*: The exclusion of planet HD 10180 h has a big influence on the outcome. Comets with initial eccentricity lower than 0.98 are no longer affected by interactions with the planets and thus stay in the system. Only the ones with initial eccentricities of > 0.98 reach the orbit of planet g and thus can be ejected from the system. *Lower right*: The calculation of the whole system (with 4 planets) for an integration time of 5 Myr shows almost the same pattern as the two panels in the *upper* row. The total number of ejected comets is higher, however, as expected.

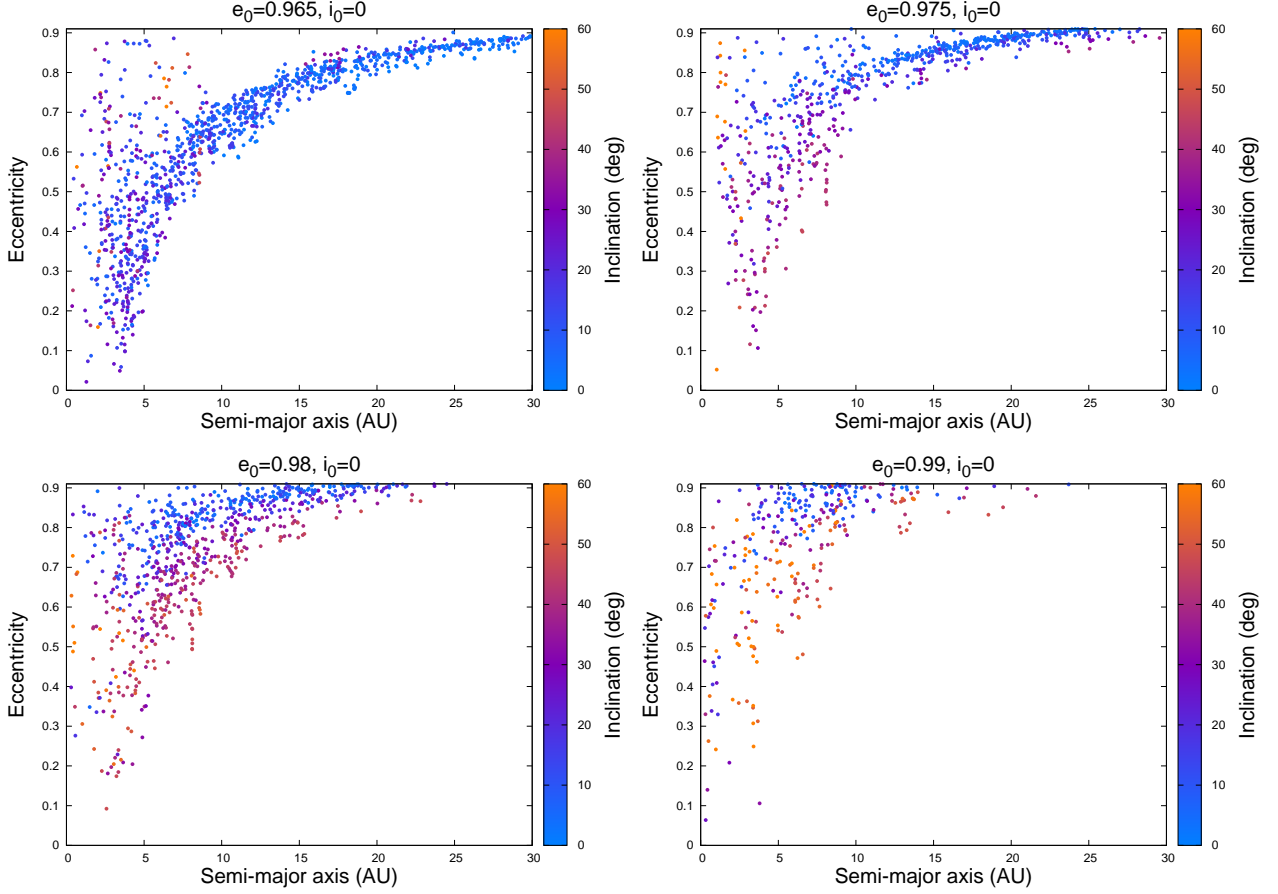


Fig. 9.— Orbital properties of captured comets with four different initial eccentricities, which are $e_0 = 0.965$, 0.975 , 0.98 , and 0.99 , and an initial inclination of $i_0 = 0^\circ$. The color scheme indicates the inclination at the time of capture. For these computations all four planets have been included and the integration time has been set to 1 Myr. Our results indicate that some comets are captured in orbits of low eccentricity and a small semi-major axis. Those comets could potentially form a *Jupiter family* analogue in the HD 10180 system. However, no clear distinction between short- and long-period comets could be identified. Nevertheless, most comets are captured in highly eccentric orbits and will probably be ejected from the system later on. The higher the initial eccentricity e_0 , the less probable it is for a comet to be captured in an orbit with moderate values for its semi-major axis and eccentricity. Interestingly, some comets, especially those with large initial eccentricity ($e_0 > 0.97$), are scattered to inclinations of up to 60° .

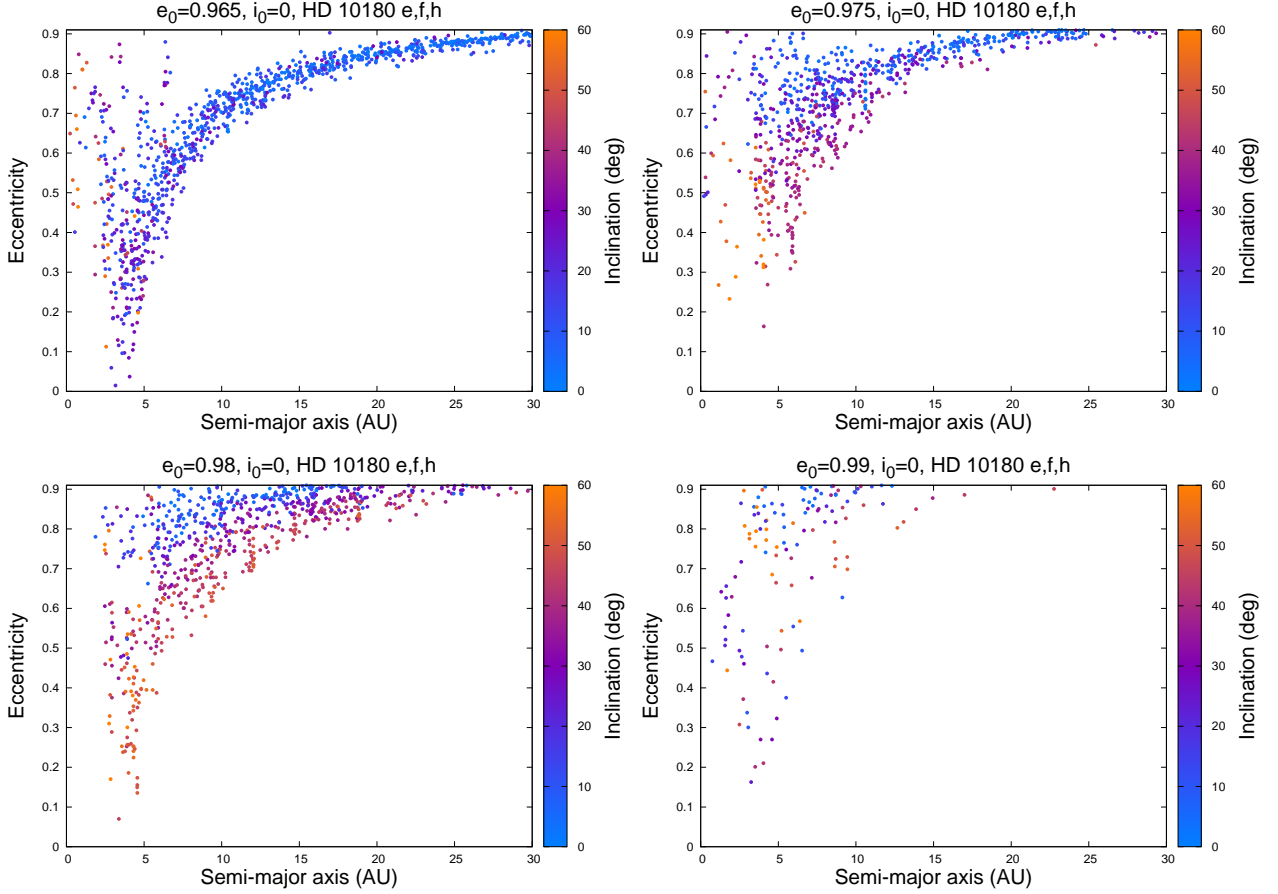


Fig. 10.— Same as Fig. 9, but with planet HD 10180 g excluded from the system. Comparing this figure with Fig. 9 with all planets included reveals similar outcomes, indicating that the influence of planet g on the orbital properties of captured comets is relatively small. Again, comets captured on close in orbits may have high inclinations, especially for comets with $e_0 < 0.97$.

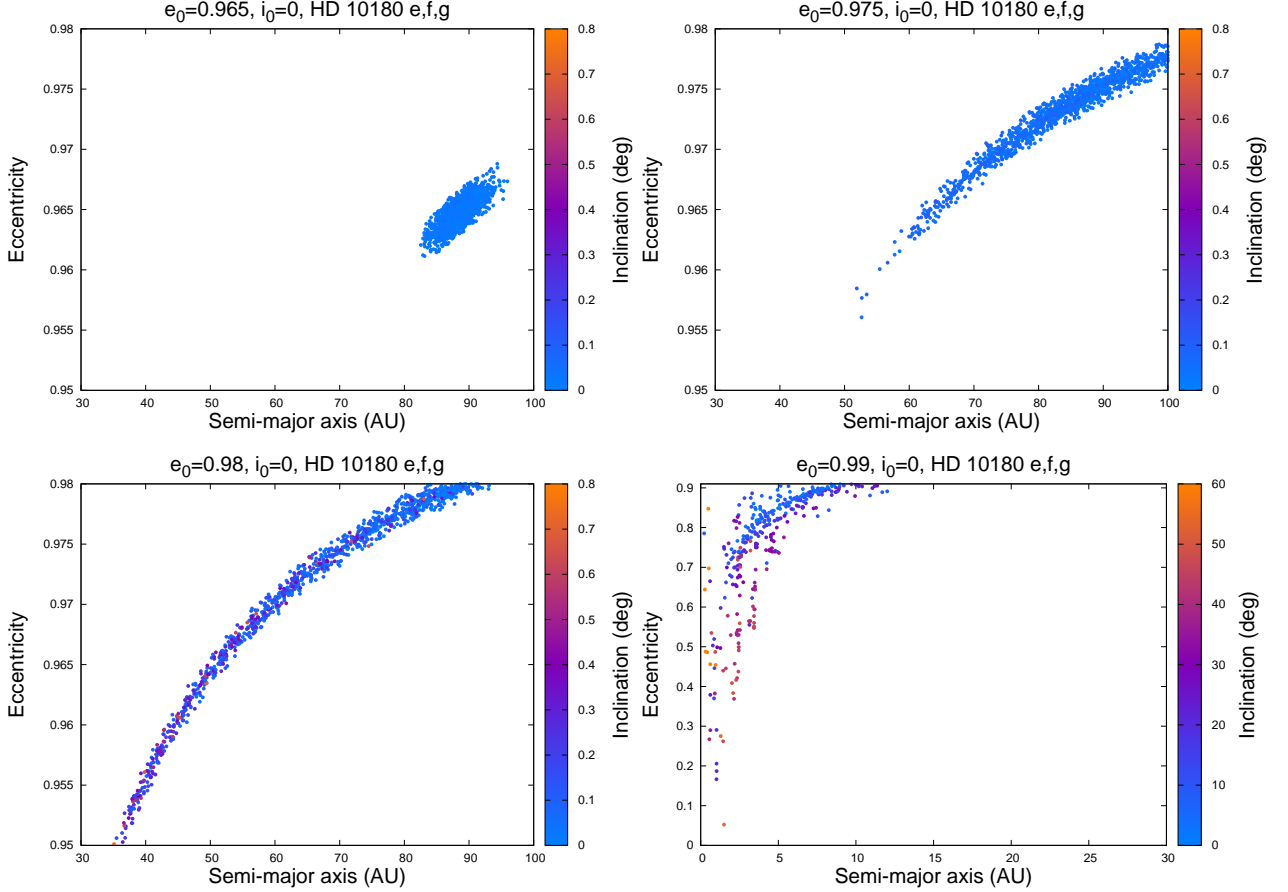


Fig. 11.— Same as Fig. 9, but with planet HD 10180 h (the most massive planet) excluded from the system. The outcome is now significantly different from the simulations with all four planets considered. Comets with initially small eccentricity do not reach the orbit of the now most massive planet of the system, HD 10180 g. Thus, they cannot interact and their orbits remain unchanged. For example, the upper left panel, pertaining to $e_0 = 0.965$, indicates that comets still populate orbits with high eccentricities and semi-major axes of $a > 80$ au akin to their initial values. (Note the range of the y -axis!) The picture changes slightly with increasing initial eccentricities, which allows comets to penetrate into the inner planetary system and to start interacting with planet HD 10180 g. For comets with initial eccentricity of $e_0 = 0.98$, it is possible for them to be captured on orbits with semi-major axes $a < 40$ au, but the eccentricity for these orbits still remains high, which makes a permanent capture unlikely. Based on the result of this figure with planet HD 10180 h omitted, as well as the comparisons to Fig. 9 and Fig. 10, we can conclude again that planet HD 10180 h definitely plays the main role in capturing comets.

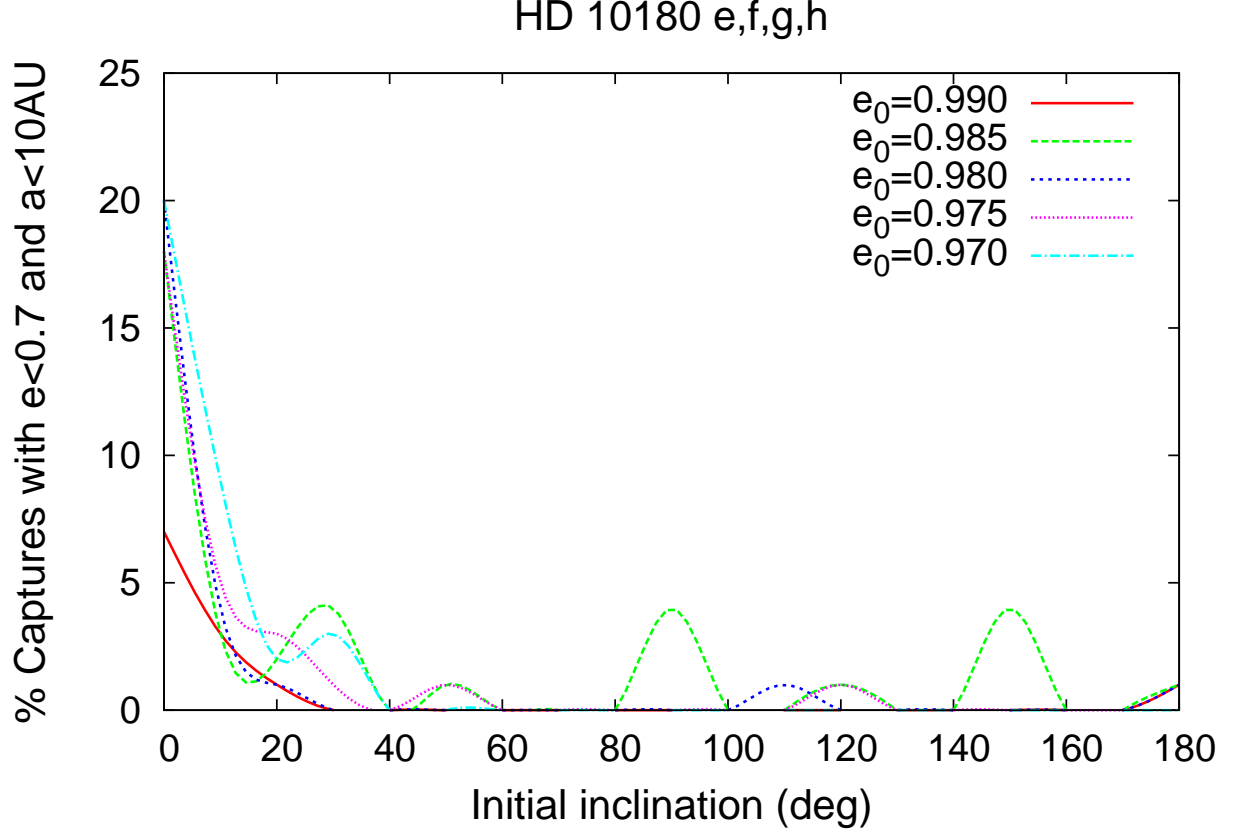


Fig. 12.— Probability for a comet with specific initial conditions (e_0, i_0) to be captured in an orbit with $e < 0.7$ and $a < 10$ au. The highest probability of capture occurs for an initial eccentricity between $e_0 = 0.97$ and 0.98 combined with an initial inclination close to 0° . The next highest peaks arise for $i_0 = 30^\circ$, $i_0 = 90^\circ$, and $i_0 = 150^\circ$. These occurrences mark initial inclinations largely coinciding with the system’s plane of orbit and perpendicular to that plane. The probability for a comet with initial eccentricity lower than $e_0 = 0.97$ is close to zero for all inclinations. Note that comets of $e_0 = 0.975$ have the highest probability to be captured.

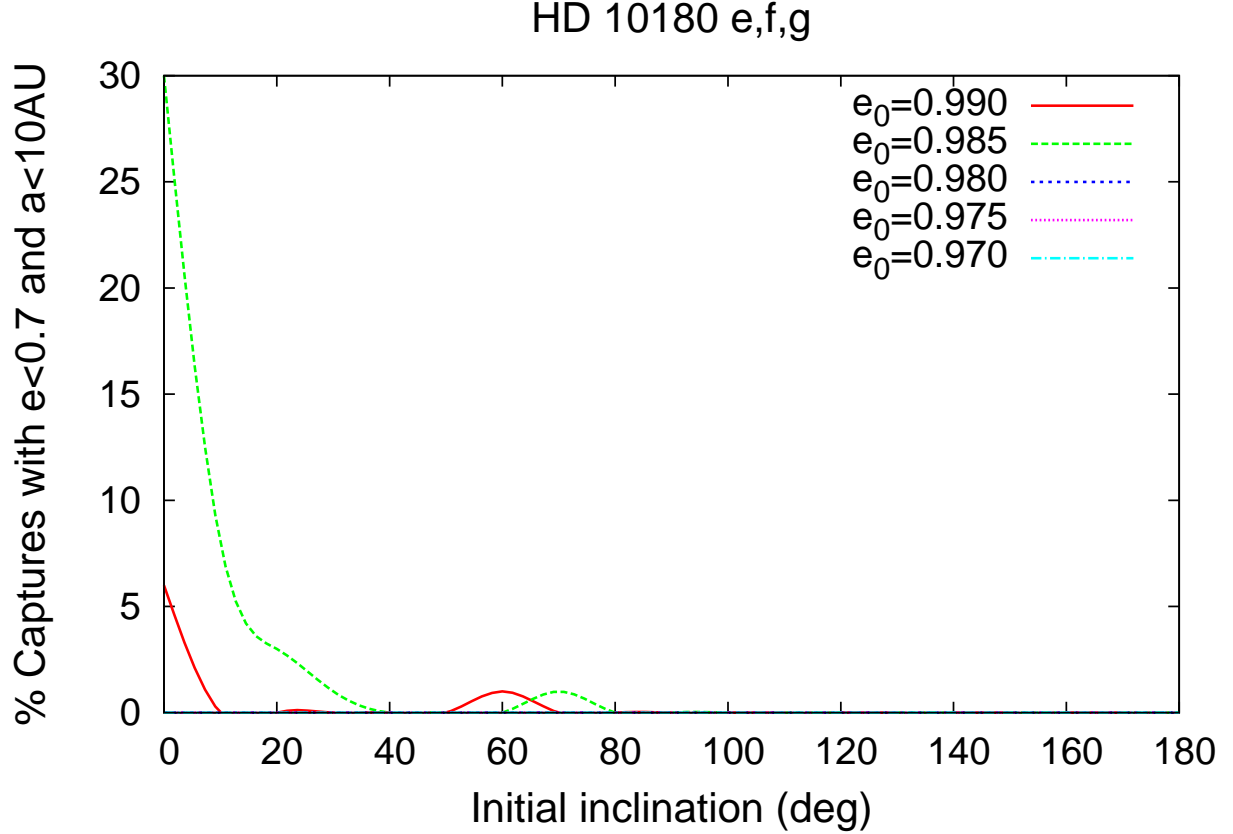


Fig. 13.— Same as Fig. 12, but without planet HD 10180 h. Interestingly, the probability for a capture into orbits with moderate values for a and e is 30% for comets with initial eccentricities of 0.985. This percentage is even higher than for models with planet h included (compare Fig. 12). Thus, we can conclude that the combination of the scattering given by planet g and h plays a prevalent role for comets with this particular initial eccentricity. Noting that the probability for a capture for comets with $e_0=0.99$ remains about the same, leads to the conclusion that for comets in highly eccentric orbits planet g plays the main role in the scattering process. On the other hand, comets with lower initial eccentricities, i.e., $e < 0.985$, have a perihelion distance beyond the orbit of planet g and thus cannot be majorly affected by this planet, which is why the probability for them to be captured is zero.

Table 1. The HD 10180 Planetary System, Part I

Name	a	e	i	ω	Ω	M	m
...	(au)	...	($^{\circ}$)	($^{\circ}$)	($^{\circ}$)	($^{\circ}$)	(M_{\odot})
HD 10180 e	0.270	0.0260	0.70	1.0	1.0	50.0	0.0000790
HD 10180 f	0.49220	0.1350	0.70	1.0	1.0	90.0	0.0000750
HD 10180 g	1.4220	0.00010	0.80	1.0	1.0	181.0	0.0000670
HD 10180 h	3.40	0.080	0.60	1.0	1.0	1.0	0.0002

Note. — The four outer planets of HD 10180, which have been included in our study. Moreover, there are three additional planets orbiting inside of HD 10180 e, as well as two unconfirmed planets; see Tuomi (2012) and <http://www.exoplanet.eu> for details and updates.

Table 2. The HD 10180 Planetary System, Part II

Name	Mass	R_{Hill}	R_{Hill}	r_{ρ_1}	r_{ρ_2}
...	(m_{Jupiter})	(au)	(10^6 km)	(10^3 km)	(10^3 km)
HD 10180 e	0.0827	0.0080	1.18	33	26
HD 10180 f	0.0786	0.0144	2.12	32	26
HD 10180 g	0.0702	0.0400	5.91	31	25
HD 10180 h	0.2095	0.1379	20.40	45	36

Note. — Masses (in m_{Jupiter}), Hill radii and planetary radii (for two different densities) for the four planets of HD 10180 considered in our integrations with assumed densities of $\rho_1 = 1 \text{ g cm}^{-3}$ and $\rho_2 = 2 \text{ g cm}^{-3}$.

Table 3. Results for Comets in Prograde Orbits, Part 1

Incl.	Eccentricity								
	...	0.905	0.910	0.915	0.920	0.925	0.930	0.935	0.940
0°		0	0	0	6	14	52	104	300
10°		0	0	0	4	7	70	91	230
20°		0	0	0	5	9	28	79	162
30°		0	0	0	0	7	29	71	128
40°		0	0	0	1	1	17	32	51
50°		0	0	0	0	0	0	0	0
60°		0	0	0	0	0	0	0	0
70°		0	0	0	0	0	0	0	0
80°		0	0	0	0	0	0	0	0
90°		0	0	0	0	0	0	0	0

Note. — Shown here is the number of comets ejected from the system for pairs of initial conditions (e_0, i_0) . The results of Fig. 5 are put in numbers here. For low initial eccentricities, all comets stayed in the system for the whole integration time of 1 Myr, whereas for high initial eccentricities, i.e., $e_0 > 0.920$, comets are more likely to be ejected. The number of ejected comets increases with increasing initial eccentricity.

Table 4. Results for Comets in Prograde Orbits, Part 2

Incl.	Eccentricity							
...	0.945	0.950	0.955	0.960	0.965	0.970	0.975	0.980
0°	542	1116	1919	2022	2530	4555	4099	4947
10°	450	1005	1686	2500	3234	3360	3243	2908
20°	337	630	947	1523	2068	1783	1535	1786
30°	219	531	797	1196	1391	1428	1399	1544
40°	191	385	548	1060	1239	1332	1136	1492
50°	2	5	30	106	184	171	116	118
60°	2	5	24	95	128	134	75	119
70°	0	5	12	64	122	102	68	93
80°	32	80	223	468	756	597	607	780
90°	0	1	8	62	75	70	48	64

Note. — Continuation of Table 3. For the high inclinations shown here, the number of ejected comets strongly increases.

Table 5. Results for Comets in Retrograde Orbits

Incl.	Eccentricity							
...	0.945	0.950	0.955	0.960	0.965	0.970	0.975	0.980
100°	0	0	4	31	58	71	33	57
110°	0	0	1	25	41	57	32	39
120°	0	0	0	23	46	40	33	49
130°	0	0	0	25	40	41	22	49
140°	0	0	0	15	28	30	21	57
150°	0	0	0	20	36	27	26	35
160°	0	0	0	9	30	25	28	40
170°	0	0	0	9	24	44	48	86

Note. — Compare Table 3 and 4. For retrograde orbits ($i_0 > 90^\circ$) the picture is qualitatively almost the same. Comets starting with initially low eccentricities tend to be stable and remain in the system. Therefore, the number of ejected comets as, e.g., for $e_0 = 0.945$ is zero for all retrograde inclinations. For increasing values of eccentricity, the number of ejected comets increases for all inclinations.